THE JOURNAL OF PHYSICAL CHEMISTRY C
A JOURNAL OF THE AMERICAN CHEMICAL SOCIETY

pubs.acs.org/JPCC

Article

Superconductivity in the Endohedral Ga Cluster Compound $PdGa_5$

Zuzanna Ryżyńska, Piotr Wiśniewski, Dariusz Kaczorowski, Weiwei Xie, Robert J. Cava, Tomasz Klimczuk, and Michał J. Winiarski*

Cite This: *J. Phys. Chem. C* 2021, 125, 11294−11299

Read Online

ACCESS | Metrics & More | Article Recommendations | Supporting Information

ABSTRACT: Superconductivity is observed below T_c = 1.6 K in an endohedral Ga cluster compound $PdGa_5$ using magnetization and heat capacity measurements. Electronic structure calculations show that the density of states (DOS) at the Fermi level is dominated by Ga *s* and *p* states and that the overall shape of DOS is similar to what was found in other endohedral Ga cluster superconductors, such as Mo_xGa_{5x+1}, $ReGa_5$, and T_2Ga_9 (*T* = Rh and Ir). Our results provide a more complete picture of the relationship between the valence electron count and superconductivity in the family of endohedral Ga cluster superconductors.

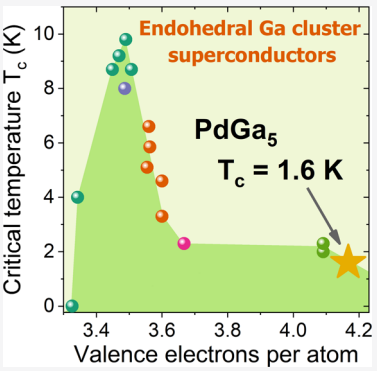

INTRODUCTION

One of the greatest challenges in research on superconducting materials is the lack of robust design guidelines that one could follow to create a superconductor by design. Due to the lack of a complete and universal theory of superconductivity, a significant amount of work has been devoted to finding empirical correlation between the chemical composition, normal (i.e., non-superconducting) state, and the occurrence of superconductivity (see, e.g., refs 1−6).

Endohedral Ga cluster compounds constitute a family of superconductors that recently gained increased attention.[7−25] While crystal structures found in the TM_xGa_y (TM, transition metal) compounds are diverse and rather complex, they can be conveniently described as networks of interconnected endohedral Ga clusters. Xie *et al.*[8] showed the correlation between the cluster connectivity and the valence electron count (VEC).

What is important for searching new superconducting materials is that endohedral Ga cluster compounds also show the relationship between the critical temperature (T_c) and VEC,[8] alike other groups of superconducting materials,[26] such as metallic elements,[1,27,28] binary A-15 phases,[1,27,29] Heusler compounds,[30,31] and high-entropy alloys.[32,33]

In the case of endohedral gallides, the highest T_c values were reported for Mo_8Ga_{41} (T_c = 9.8 K) and Mo_6Ga_{31} (T_c = 8.0 K) with VEC ≈ 21.4 and 21.5 per transition metal atom, respectively.[8] For a larger VEC, the critical temperatures are much lower, namely, T_c = 2.3 K for $ReGa_5$ (VEC = 22) and T_c = 2.0 for Rh_2Ga_9 (VEC = 22.5).[7,8]

$PdGa_5$ is an endohedral cluster compound that has 25 valence electrons and a mixed edge- and vertex-sharing manner of cluster connection. The unit cell of $PdGa_5$ with clusters of gallium around palladium atoms is shown in Figure 1. Each Pd atom is surrounded by 10 Ga atoms. Pd atoms in $PdGa_5$ are well separated with the closest Pd−Pd distance of ca. 4.6 Å; thus, direct Pd−Pd bonding is negligible. Such a situation is also found in other endohedral Ga cluster superconductors, such as Mo_8Ga_{41},[15,20,34,35] Mo_6Ga_{31},[22,36] Mo_4Ga_{21},[14,17] and TM_2Ga_9[7] families. However in $ReGa_5$,[8] the Re−Re distance is clearly within the direct bonding range. The $PdGa_{10}$ units form a three-dimensional vertex-sharing network with sizable voids between the clusters. The crystal structure of $PdGa_5$ has been thoroughly studied and discussed by Grin *et al.*[37]

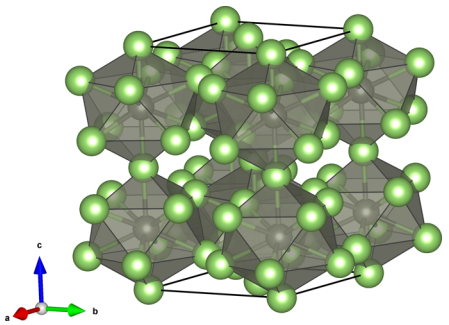

Figure 1. Unit cell of $PdGa_5$ (Ga atoms, green; Pd, gray). Vertex-sharing $PdGa_{10}$ clusters are shown in gray.

Received: April 22, 2021
Revised: May 3, 2021
Published: May 17, 2021

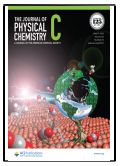

https://doi.org/10.1021/acs.jpcc.1c03615
J. Phys. Chem. C 2021, 125, 11294−11299

The number of valence electrons per transition metal atom situates $PdGa_5$ in the rightmost part of the T_c vs VEC diagram proposed by Xie *et al.*[8] with no superconducting transition down to 1.8 K.

In this work, we have revisited $PdGa_5$ to investigate its properties below 1.8 K. Flux-grown single crystals of this material were examined by means of magnetic susceptibility and heat capacity measurements. The compound was found to superconduct below T_c = 1.6 K, thus supporting the VEC-T_c relationship suggested for the endohedral gallide materials.

MATERIALS AND METHODS

Single crystals of $PdGa_5$ were synthesized using the self-flux method.[38] Palladium powder (Mennica-Metale, Poland, 99.95%) and pieces of a gallium ingot (Alfa Aesar, 99.99%) were inserted into an alumina crucible in a 3:22 molar ratio. Another crucible and a frit disk were used to facilitate the separating flux from the crystals.[39] The set was closed in a quartz ampoule filled with Ar gas. The ampoule was placed in a box furnace, heated up to 300 °C, kept at this temperature for 12 h, and cooled with a rate of 1 °C/h down to 100 °C. At this temperature, the excess flux was centrifuged. The crystals obtained were small (about 0.5 mm in the longest dimension), silver, and shiny. As the masses of individual crystals were not sufficient, clusters of randomly oriented single crystals were used for measurements of physical properties (magnetization and heat capacity).

Powder X-ray diffraction (PXRD) was performed using a Bruker D8 Focus diffractometer with Cu K_α radiation on several single crystals crushed and fine-ground in an agate mortar. LeBail profile matching, performed using the FullProf package,[40] confirmed the tetragonal structure of $PdGa_5$.

Magnetic susceptibility and magnetization measurements were carried out in the temperature range of 0.5−1.6 K and in magnetic fields up to $\mu_0 H$ = 10 mT employing a Quantum Design MPMS-XL superconducting quantum interference device (SQUID) magnetometer equipped with a ^{3}He refrigerator.

Heat capacity measurements were done in the temperature range of 0.5−3 K in applied magnetic fields up to $\mu_0 H$ = 10 mT using a Quantum Design physical property measurement system (PPMS) with a dilution refrigerator option employing the semi-adiabatic pulse technique.

Electronic structure calculations were done with the Quantum Espresso package[41−43] employing the projector-augmented wave (PAW)[44,45] sets from the PSlib database[46] and the Perdew−Burke−Ernzerhof generalized gradient approximation[47] exchange-correlation potential. Wave function and charge density cutoffs were set to 62 and 500 Ry, respectively. The experimental primitive cell dimensions and atomic positions were relaxed using the Broyden−Fletcher−Goldfarb−Shanno algorithm. For calculations, a 6 × 6 × 7 k-point mesh was used. The symmetrized unit cell parameters were calculated from the relaxed primitive cell using the FINDSYM program of the ISOTROPY suite[48] (see Table S1 of the Supporting Information). Crystal orbital Hamilton population (COHP)[49,50] analysis was performed using the LOBSTER code.[51]

RESULTS AND DISCUSSION

The measured PXRD pattern of $PdGa_5$ is presented in Figure 2. All of the observed reflections can be indexed with a tetragonal (space group $I4/mcm$) unit cell. The detailed results of the LeBail refinement are given in Table S2 of the Supporting Information. The derived unit cell parameters a = 6.4347(1) Å and c = 9.9871(2) Å are in good agreement with the values reported by Grin *et al.*[S2]

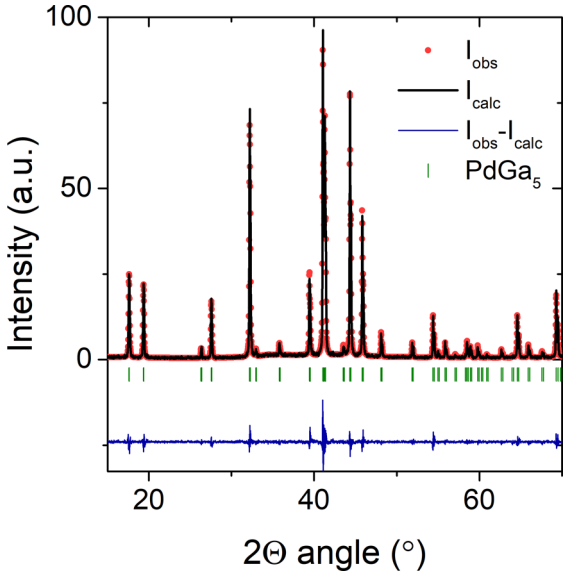

Figure 2. PXRD pattern for crushed $PdGa_5$ single crystals. Observed data are marked with red dots. The LeBail fit is presented as black solid lines, and the difference between the observed and calculated profile is shown with blue lines. Bragg positions are marked with green ticks.

The results of magnetization measurements are presented in Figure 3a−d. The low-temperature zero-field-cooled (ZFC) and field-cooled (FC) magnetic susceptibility data are shown in Figure 3a. After accounting for the demagnetization effect (discussed below), the ZFC susceptibility χ_V at T = 0.5 K is close to $-1/4\pi$, showing that the sample is in a fully diamagnetic (Meissner) state. The bifurcation between the ZFC and FC curves indicates a magnetic flux pinning on crystal defects. The critical temperature, determined from the ZFC data as a point at which the steepest slope of $\chi_V(T)$

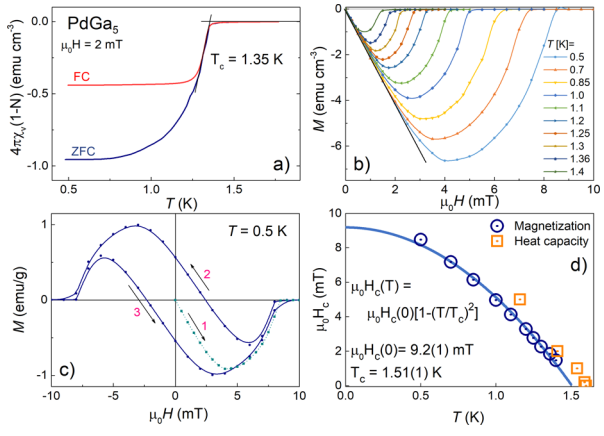

Figure 3. Magnetic data of PdGa5. (a) ZFC and FC magnetic susceptibility measured in $\mu_0 H$ = 2 mT, (b) magnetization isotherms, (c) hysteresis loop taken at T = 0.5 K, and (d) critical field vs temperature, obtained from magnetization (blue) and heat capacity (orange) data.

https://doi.org/10.1021/acs.jpcc.1c03615
J. Phys. Chem. C 2021, 125, 11294−11299

intersects the normal state susceptibility,[53] amounts to T_c = 1.35 K. This value is somewhat smaller than that obtained from a zero-field heat capacity measurement (see below) because of the rather low critical field in $PdGa_5$.

The sample demagnetization factor N is determined using the data shown in Figure 3b. The points collected at the lowest temperature were fitted with a linear function $M = aH + b$ (black solid line), assuming a perfect diamagnetic response. From the equation $-a = \frac{1}{4\pi(1-N)}$, N = 0.62 was derived, in a reasonable agreement with the sample geometry.[54] The field values at which the susceptibility reaches zero (suppression of the Meissner state) were taken as the critical fields $\mu_0 H_c(T)$ and plotted as a function of temperature, as shown in Figure 3d. The so-obtained data were fitted with the formula $\mu_0 H_c(T) = \mu_0 H_c(0)[1 - (T/T_c)^2]$ (orange solid line), yielding $\mu_0 H_c(0)$ = 9.2(1) mT. The critical temperature estimated from the same fit is T_c = 1.51 K, i.e., close to the value determined from the heat capacity data (see below). Figure 3c presents the magnetization isotherm taken at T = 0.5 K. The shape of the M vs H loop differs from what one expects for a typical type-II superconductor but is consistent with type-I superconductivity with significant contribution of demagnetization effects (see, e.g., ref 55).

The results of heat capacity measurements are shown in Figure 4a,b. From the equal entropy construction procedure shown in Figure 4a, the critical temperature was determined as T_c = 1.6 K, and the superconducting jump was estimated to be $\Delta C_p/T_c$ = 6.49 mJ mol^{-1} K^{-2}. As can be inferred from Figure 4c, the C_p anomaly is suppressed by the external magnetic field in a manner consistent with the magnetization data (see Figure 3).

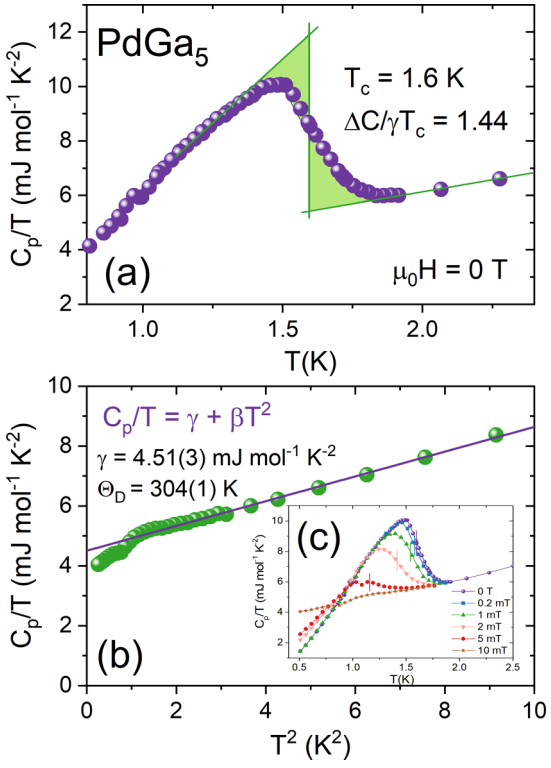

Figure 4. Heat capacity data for PdGa5. (a) Equal entropy analysis of the superconducting anomaly. (b) Normal state specific heat (in an applied field of $\mu_0 H$ = 10 mT) described by the low-temperature expansion of the Debye model (solid straight line). Inset (c): low-temperature specific heat measured in different applied magnetic fields.

In the normal state (the data were measured in $\mu_0 H$ = 10 mT), the heat capacity of $PdGa_5$ can be described with the Debye formula $C_p/T = \gamma + \beta T^2$, where γ is the Sommerfeld electronic coefficient and the second term accounts for the phonon contribution. The least-squares fit shown in Figure 4b yields γ = 4.51(3) mJ mol^{-1} K^{-2} and β = 0.413(6) mJ mol^{-2} K^{-4}. Using the relation

$$\Theta_D = \sqrt[3]{\frac{12\pi^4 nR}{5\beta}}$$

where n is the number of atoms per formula unit (here, n = 6) and R is the gas constant (R = 8.31 J mol^{-1} K^{-1}); one finds the Debye temperature Θ_D = 304(1) K. Notably, the normalized heat capacity jump $\Delta C_p/\gamma T_c$ = 1.44 estimated for $PdGa_5$ is very close to the value predicted by the Bardeen–Cooper–Schrieffer (BCS) theory for the weak-coupling limit.

Taking the Θ_D and T_c values estimated from the heat capacity measurement and using the inverted McMillan formula[56]

$$\lambda_{el\text{-}ph} = \frac{1.04 + \mu^* \ln\left(\frac{\Theta_D}{1.45T_c}\right)}{(1 - 0.62\mu^*)\ln\left(\frac{\Theta_D}{1.45T_c}\right) - 1.04}$$

where μ^* is the Coulomb pseudopotential parameter (in typical superconductors, μ^* usually equals to 0.10–0.15; here, μ^* = 0.13 was assumed), the electron–phonon coupling constant was estimated as $\lambda_{el\text{-}ph}$ = 0.49, indicative of the weak coupling regime.

As depicted in Figure 5a, the electronic density of states at the Fermi energy E_F is dominated by Ga s and p orbitals with

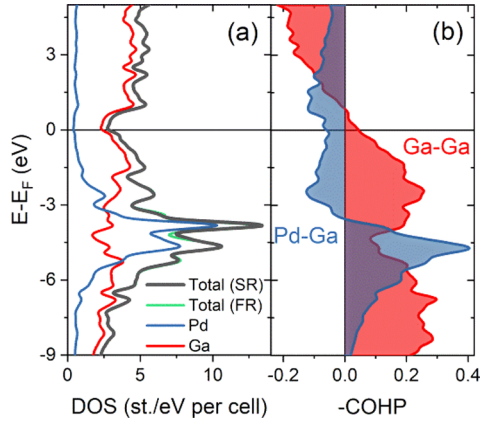

Figure 5. Density of states (a) and crystal orbital Hamilton population (b) calculated for $PdGa_5$. The COHP curves are shown as an average over all Pd–Ga (20 per cell) or Ga–Ga pairs (36 per cell).

only about 14% contribution due to Pd atoms. The Pd d states are mostly occupied, lying over 3 eV below E_F. Remarkably, the Fermi level in $PdGa_5$ is situated within a pseudogap.

Despite structural differences, the overall character of the DOS is remarkably similar to other endohedral Ga cluster superconductors.[8,10,57,58] In each of them, transition metal d states are almost fully occupied, being located 2–3 eV below

https://doi.org/10.1021/acs.jpcc.1c03615
J. Phys. Chem. C 2021, 125, 11294–11299

E_F. This similarity of the electronic structures allows comparing this structurally diverse group on a common basis of the valence electron count.

The COHP calculations (Figure 5b) show that the DOS (E_F) has a significant contribution of Pd−Ga antibonding states (−COHP <0 above −3 eV), while Ga−Ga interactions have (on average) a bonding character up to ca. 0.5 eV above E_F. In our recent study of an endohedral Al superconductor $RuAl_6$, we demonstrated that the occupation of antibonding states results in an electronic structure instability, in this case manifesting itself as a superconducting transition.[59] Thus, a slight electron doping of $PdGa_5$, shifting E_F toward the Ga−Ga antibonding range, may result in an increase of T_c.

The total VEC in $PdGa_5$ is 25 per Pd, equivalent to ca. 4.17 per atom, making this material the most electron-rich endohedral Ga cluster compound. A number of endohedral Ga superconductors were reported since Xie *et al.*[8] have suggested the relationship between T_c and VEC per TM atom.[10,14,15,17] Inclusion of these recently reported phases provides further support for that correlation (see Figure 6a).

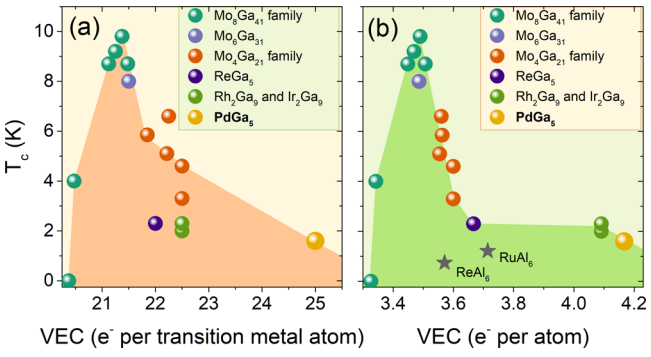

Figure 6. Relationship between the T_c and valence electron count in endohedral gallide superconductors. Within the Mo_8Ga_{41} family, the VEC was changed by partial substitution in both Mo (with V)[11,20] and Ga sites (with Sn and Zn).[13−15] The Mo_4Ga_{21} family consists of five reported members with Ga partially substituted by chalcogens, Sn, or Sb.[14,17] In panel (a), the total number of valence electrons is divided by the number of transition metal atoms (VEC/TM atom, as was proposed by Xie *et al.*).[8] Panel (b) shows the VEC divided by the total number of atoms (VEC/atom). Two endohedral aluminide superconductors, $RuAl_6$ (T_c = 1.2 K)[59] and $ReAl_6$ (T_c = 0.74 K),[60] are also included in panel (b) for comparison.

However, most of the known superconducting Ga endohedral cluster compounds have only up to 22.5 electrons per TM atom, limiting the possibility to extend the conclusions to $PdGa_5$ with VEC/TM atom = 25.

If the T_c data is plotted against the VEC divided per total number of atoms (see Figure 6b), then $PdGa_5$ lies close to Rh_2Al_9 and Ir_2Al_9 compounds with slightly higher T_c = 2.0 and 2.3 K, respectively. Remarkably, in such a representation, $ReGa_5$ seems to follow an almost linear decrease of T_c between VEC = 3.49 per atom (Mo_8Ga_{41}, T_c = 9.8) and VEC = 3.67 per atom ($ReGa_5$, T_c = 2.3 K).

No endohedral Ga cluster superconductors are known with VEC/atom values between 3.67 and 4.09. In our recent study on $RuAl_6$ (VEC/atom = 3.71), we suggested that electron doping might increase its T_c.[59] In the case of $PdGa_5$, the VEC-T_c correlation shown in Figure 6a,b would suggest that electron doping should reduce the T_c, but superconductivity can possibly be enhanced by hole doping. The synthesis and characterization of electron-doped $ReGa_5$ or hole-doped TM_2Ga_9 and $PdGa_5$ are thus of high interest as they could provide further data to elucidate the relationship between T_c and VEC over a broader range.

CONCLUSIONS

We have studied the low-temperature properties of the endohedral Ga cluster compound $PdGa_5$ and found it to become superconducting below T_c = 1.6 K. The low critical field and the shape of the $M(H)$ loop suggest that $PdGa_5$ is a type-I superconductor, but further studies are necessary to elucidate this point.

The electronic structure calculations revealed that, despite structural differences, $PdGa_5$ is similar to other endohedral Ga cluster superconductors. The observed T_c value fits into the VEC-T_c correlation suggested before for this family,[8] highlighting its robustness. Electron and hole doping experiments on $ReGa_5$, TM_2Ga_9, and $PdGa_5$ should provide further insight into the observed VEC-T_c relationship.

ASSOCIATED CONTENT

Supporting Information

The Supporting Information is available free of charge at https://pubs.acs.org/doi/10.1021/acs.jpcc.1c03615.

Results of LeBail analysis of PXRD data and DFT-relaxed structural parameters for $PdGa_5$ (PDF)

AUTHOR INFORMATION

Corresponding Author

Michał J. Winiarski − *Faculty of Applied Physics and Mathematics and Advanced Materials Center, Gdansk University of Technology, Gdansk 80-232, Poland;* orcid.org/0000-0001-9083-8066; Email: michal.winiarski@pg.edu.pl

Authors

Zuzanna Ryżyńska − *Faculty of Applied Physics and Mathematics and Advanced Materials Center, Gdansk University of Technology, Gdansk 80-232, Poland*

Piotr Wiśniewski − *Institute of Low Temperature and Structure Research, Polish Academy of Sciences, Wrocław 50-422, Poland*

Dariusz Kaczorowski − *Institute of Low Temperature and Structure Research, Polish Academy of Sciences, Wrocław 50-422, Poland*

Weiwei Xie − *Department of Chemistry and Chemical Biology, Rutgers University, Piscataway, New Jersey 08854, United States;* orcid.org/0000-0002-5500-8195

Robert J. Cava − *Department of Chemistry, Princeton University, Princeton, New Jersey 08544, United States*

Tomasz Klimczuk − *Faculty of Applied Physics and Mathematics and Advanced Materials Center, Gdansk University of Technology, Gdansk 80-232, Poland;* orcid.org/0000-0002-7089-4631

Complete contact information is available at: https://pubs.acs.org/10.1021/acs.jpcc.1c03615

Author Contributions

The manuscript was written through contributions of all authors.

Notes

The authors declare no competing financial interest.

■ ACKNOWLEDGMENTS

The research at GUT was supported by the National Science Centre (Poland) grant (UMO 2018/29/N/ST5/01286). The work done at Rutgers was supported by the Beckman Young Investigator Award. The analysis of the results at Princeton was supported by the U.S. Department of Energy, Division of Basic Energy Sciences, grant DE-FG02-98ER45706.

■ ABBREVIATIONS

COHP, crystal orbital Hamilton population; DOS, density of (electronic) states; FC, field-cooled; PXRD, powder X-ray diffraction; SC, superconductor; TM, transition metal; VEC, valence electron count; ZFC, zero-field-cooled

■ REFERENCES

(1) Matthias, B. T. Empirical Relation between Superconductivity and the Number of Valence Electrons per Atom. *Phys. Rev.* **1955**, *97*, 74−76.
(2) Hirsch, J. E. Correlations between Normal-State Properties and Superconductivity. *Phys. Rev. B* **1997**, *55*, 9007−9024.
(3) Stanev, V.; Oses, C.; Kusne, A. G.; Rodriguez, E.; Paglione, J.; Curtarolo, S.; Takeuchi, I. Machine Learning Modeling of Superconducting Critical Temperature. *npj Comput. Mater.* **2018**, *4*, 29.
(4) Gaikwad, M.; Doke, A. R. Featureless Approach for Predicting Critical Temperature of Superconductors. In *2020 11th International Conference on Computing, Communication and Networking Technologies (ICCCNT)*; IEEE, *2020*; pp. 1−5.
(5) Roter, B.; Dordevic, S. V. Predicting New Superconductors and Their Critical Temperatures Using Machine Learning. *Phys. C* **2020**, *575*, 1353689.
(6) Torshin, I. Y.; Rudakov, K. V. Topological Data Analysis in Materials Science: The Case of High-Temperature Cuprate Superconductors. *Pattern Recognit. Image Anal.* **2020**, *30*, 264−276.
(7) Takeda, M.; Teruya, A.; Nakamura, A.; Harima, H.; Hedo, M.; Nakama, T.; Ōnuki, Y. De Haas−van Alphen Effect in Rh2Ga9 and Ir2Ga9 without Inversion Symmetry in the Crystal Structure and Related Compounds T2Al9 (T: Co, Rh, Ir) with Inversion Symmetry. *J. Phys. Soc. Jpn.* **2014**, *84*, No. 024701.
(8) Xie, W.; Luo, H.; Phelan, B. F.; Klimczuk, T.; Cevallos, F. A.; Cava, R. J. Endohedral Gallide Cluster Superconductors and Superconductivity in ReGa5. *Proc. Natl. Acad. Sci. U. S. A.* **2015**, *112*, E7048−E7054.
(9) Sumiyama, A.; Kawakatsu, D.; Gouchi, J.; Kawasaki, I.; Yamaguchi, A.; Motoyama, G.; Hirose, Y.; Settai, R.; Ōnuki, Y. Search for Spontaneous Magnetization in Noncentrosymmetric Superconductors. *J. Phys.: Conf. Ser.* **2016**, *683*, No. 012029.
(10) Verchenko, V. Y.; Tsirlin, A. A.; Zubtsovskiy, A. O.; Shevelkov, A. V. Strong Electron-Phonon Coupling in the Intermetallic Superconductor Mo8Ga41. *Phys. Rev. B* **2016**, *93*, No. 064501.
(11) Verchenko, V. Y.; Khasanov, R.; Guguchia, Z.; Tsirlin, A. A.; Shevelkov, A. V. Two-Gap Superconductivity in Mo8Ga41 and Its Evolution upon Vanadium Substitution. *Phys. Rev. B* **2017**, *96*, 134504.
(12) Neha, P.; Sivaprakash, P.; Ishigaki, K.; Kalaiselvan, G.; Manikandan, K.; Dhaka, R. S.; Uwatoko, Y.; Arumugam, S.; Patnaik, S. Nuanced Superconductivity in Endohedral Gallide Mo8Ga41. *Mater. Res. Express* **2019**, *6*, No. 016002.
(13) Verchenko, V. Y.; Mironov, A. V.; Wei, Z.; Tsirlin, A. A.; Dikarev, E. V.; Shevelkov, A. V. Crystal Growth of Intermetallics from the Joint Flux: Exploratory Synthesis through the Control of Valence Electron Count. *Inorg. Chem.* **2019**, *58*, 1561−1570.
(14) Verchenko, V. Y.; Zubtsovskii, A. O.; Wei, Z.; Tsirlin, A. A.; Marcin, M.; Sobolev, A. V.; Presniakov, I. A.; Dikarev, E. V.; Shevelkov, A. V. Endohedral Cluster Superconductors in the Mo−Ga−Sn System Explored by the Joint Flux Technique. *Inorg. Chem.* **2019**, *58*, 15552−15561.
(15) Verchenko, V. Y.; Zubtsovskii, A. O.; Wei, Z.; Tsirlin, A. A.; Dikarev, E. V.; Shevelkov, A. V. From Endohedral Cluster Superconductors to Approximant Phases: Synthesis, Crystal and Electronic Structure, and Physical Properties of Mo 8 Ga 41−x Zn x and Mo 7 Ga 52−x Zn x. *Dalton Trans.* **2019**, *48*, 7853−7861.
(16) Sirohi, A.; Saha, S.; Neha, P.; Das, S.; Patnaik, S.; Das, T.; Sheet, G. Multiband Superconductivity in Mo8Ga41 Driven by a Site-Selective Mechanism. *Phys. Rev. B* **2019**, *99*, No. 054503.
(17) Verchenko, V. Y.; Zubtsovskii, A. O.; Plenkin, D. S.; Bogach, A. V.; Wei, Z.; Tsirlin, A. A.; Dikarev, E. V.; Shevelkov, A. V. Family of Mo4Ga21-Based Superconductors. *Chem. Mater.* **2020**, *32*, 6730−6735.
(18) Zhou, Y.; Zhou, Y.; Chen, C.; Chen, X.; An, C.; Zhang, L.; Wu, W.; Zhang, Z.; Yang, Z. Pressure Tuning of Superconductivity in Mo8Ga41 Single Crystals. *Phys. Rev. B* **2020**, *102*, 134512.
(19) Hu, Z.; Graf, D.; Liu, Y.; Petrovic, C. Three-Dimensional Fermi Surface and Small Effective Masses in Mo8Ga41. *Appl. Phys. Lett.* **2020**, *116*, 202601.
(20) Marcin, M.; Pribulová, Z.; Kačmarčík, J.; Verchenko, V. Y.; Shevelkov, A. V.; Cambel, V.; Šoltýs, J.; Samuely, P. Local Magnetometry of Superconducting Mo8Ga41 and Mo7VGa41: Vortex Pinning Study. *Acta Phys. Pol. A.* **2020**, *137*, 794−796.
(21) Zhang, W.; Hu, Y. J.; Kuo, C. N.; Kuo, S. T.; Fang, Y.-W.; Lai, K. T.; Liu, X. Y.; Yip, K. Y.; Sun, D.; Balakirev, F. F.; et al. Linear Magnetoresistance with a Universal Energy Scale in the Strong-Coupling Superconductor Mo8Ga41 without Quantum Criticality. *Phys. Rev. B* **2020**, *102*, 241113.
(22) Verchenko, V. Y.; Zubtsovskii, A. O.; Tsirlin, A. A.; Wei, Z.; Roslova, M.; Dikarev, E. V.; Shevelkov, A. V. Mo6Ga31 Endohedral Cluster Superconductor. *J. Alloys Compd.* **2020**, *848*, 156400.
(23) Verchenko, V. Y.; Tsirlin, A. A.; Shevelkov, A. V. Semiconducting and Superconducting Mo−Ga Frameworks: Total Energy and Chemical Bonding. *Inorg. Chem. Front.* **2021**, *8*, 1702−1709.
(24) Marcin, M.; Pribulová, Z.; Kačmarčík, J.; Medvecká, Z.; Klein, T.; Verchenko, V. Y.; Cambel, V.; Šoltýs, J.; Samuely, P. One or Two Gaps in Mo8Ga41 Superconductor? Local Hall-Probe Magnetometry Study. *Supercond. Sci. Technol.* **2021**, *34*, No. 035017.
(25) Verchenko, V. Y.; Shevelkov, A. V. Endohedral Cluster Intermetallic Superconductors: At the Frontier between Chemistry and Physics. *Dalton Trans.* **2021**, *50*, 5109−5114.
(26) Poole, C. P., Jr.; Farach, H. A. Tabulations and Correlations of Transition Temperatures of Classical Superconductors. *J. Supercond.* **2000**, *13*, 47−60.
(27) Matthias, B. T. Transition Temperatures of Superconductors. *Phys. Rev.* **1953**, *92*, 874−876.
(28) Slocombe, D. R.; Kuznetsov, V. L.; Grochala, W.; Williams, R. J. P.; Edwards, P. P. Superconductivity in Transition Metals. *Phil. Trans. R. Soc. A* **2015**, *373*, 20140476.
(29) Poole, C. K.; Farach, H. A.; Creswick, R. J. *Handbook of Superconductivity*; Elsevier, 1999.
(30) Klimczuk, T.; Wang, C. H.; Gofryk, K.; Ronning, F.; Winterlik, J.; Fecher, G. H.; Griveau, J.-C.; Colineau, E.; Felser, C.; Thompson, J. D.; et al. Superconductivity in the Heusler Family of Intermetallics. *Phys. Rev. B* **2012**, *85*, 174505.
(31) Kautzsch, L.; Mende, F.; Fecher, G. H.; Winterlik, J.; Felser, C. Are AuPdTM (T = Sc, Y and M = Al, Ga, In), Heusler Compounds Superconductors without Inversion Symmetry? *Materials* **2019**, *12*, 2580.
(32) von Rohr, F.; Winiarski, M. J.; Tao, J.; Klimczuk, T.; Cava, R. J. Effect of Electron Count and Chemical Complexity in the Ta-Nb-Hf-Zr-Ti High-Entropy Alloy Superconductor. *Proc. Natl. Acad. Sci. U. S. A.* **2016**, *113*, E7144−E7150.
(33) Kitagawa, J.; Hamamoto, S.; Ishizu, N. Cutting Edge of High-Entropy Alloy Superconductors from the Perspective of Materials Research. *Metals* **2020**, *10*, 1078.
(34) Bezinge, A.; Yvon, K.; Decroux, M.; Muller, J. On the Existence of Binary Mo8Ga41 and Its Properties. *J. Less-Common Met.* **1984**, *99*, L27−L31.

https://doi.org/10.1021/acs.jpcc.1c03615
J. Phys. Chem. C 2021, 125, 11294−11299

(35) Yvon, K. Mo8Ga41, Another Example of Ten-Coordination of the Transition Element. *Acta Cryst. B* **1975**, *31*, 117−120.
(36) Yvon, K. The Crystal Structure of Mo6Ga31, a Hypersymmetrical Structure Solved by Direct Methods. *Acta Cryst. B* **1974**, *30*, 853−861.
(37) Grin, Y.; Wedig, U.; Wagner, F.; von Schnering, H. G.; Savin, A. The Analysis of "Empty Space" in the PdGa5 Structure. *J. Alloys Compd.* **1997**, *255*, 203−208.
(38) Canfield, P. C.; Fisk, Z. Growth of Single Crystals from Metallic Fluxes. *Philos. Mag. B* **1992**, *65*, 1117−1123.
(39) Canfield, P. C.; Kong, T.; Kaluarachchi, U. S.; Jo, N. H. Use of Frit-Disc Crucibles for Routine and Exploratory Solution Growth of Single Crystalline Samples. *Philos. Mag.* **2016**, *96*, 84−92.
(40) Rodríguez-Carvajal, J. Recent Advances in Magnetic Structure Determination by Neutron Powder Diffraction. *Phys. B* **1993**, *192*, 55−69.
(41) Giannozzi, P.; Baroni, S.; Bonini, N.; Calandra, M.; Car, R.; Cavazzoni, C.; Ceresoli, D.; Chiarotti, G. L.; Cococcioni, M.; Dabo, I.; et al. QUANTUM ESPRESSO: A Modular and Open-Source Software Project for Quantum Simulations of Materials. *J. Phys.: Condens. Matter* **2009**, *21*, 395502.
(42) Giannozzi, P.; Andreussi, O.; Brumme, T.; Bunau, O.; Nardelli, M. B.; Calandra, M.; Car, R.; Cavazzoni, C.; Ceresoli, D.; Cococcioni, M.; et al. Advanced Capabilities for Materials Modelling with Quantum ESPRESSO. *J. Phys.: Condens. Matter* **2017**, *29*, 465901.
(43) Giannozzi, P.; Baseggio, O.; Bonfà, P.; Brunato, D.; Car, R.; Carnimeo, I.; Cavazzoni, C.; de Gironcoli, S.; Delugas, P.; Ferrari Ruffino, F.; et al. Quantum ESPRESSO toward the Exascale. *J. Chem. Phys.* **2020**, *152*, 154105.
(44) Blöchl, P. E. Projector Augmented-Wave Method. *Phys. Rev. B* **1994**, *50*, 17953−17979.
(45) Kresse, G.; Joubert, D. From Ultrasoft Pseudopotentials to the Projector Augmented-Wave Method. *Phys. Rev. B* **1999**, *59*, 1758−1775.
(46) Dal Corso, A. Pseudopotentials Periodic Table: From H to Pu. *Comput. Mater. Sci.* **2014**, *95*, 337−350.
(47) Perdew, J. P.; Burke, K.; Ernzerhof, M. Generalized Gradient Approximation Made Simple. *Phys. Rev. Lett.* **1996**, *77*, 3865−3868.
(48) Stokes, H. T.; Hatch, D. M. FINDSYM: Program for Identifying the Space-Group Symmetry of a Crystal. *J. Appl. Crystallogr.* **2005**, *38*, 237−238.
(49) Dronskowski, R.; Bloechl, P. E. Crystal Orbital Hamilton Populations (COHP): Energy-Resolved Visualization of Chemical Bonding in Solids Based on Density-Functional Calculations. *J. Phys. Chem.* **1993**, *97*, 8617−8624.
(50) Steinberg, S.; Dronskowski, R. The Crystal Orbital Hamilton Population (COHP) Method as a Tool to Visualize and Analyze Chemical Bonding in Intermetallic Compounds. *Crystals* **2018**, *8*, 225.
(51) Maintz, S.; Deringer, V. L.; Tchougréeff, A. L.; Dronskowski, R. LOBSTER: A Tool to Extract Chemical Bonding from Plane-Wave Based DFT. *J. Comput. Chem.* **2016**, *37*, 1030−1035.
(52) Grin, Y.; Peters, K.; von Schnering, H. G. Refinement of the Crystal Structure of Palladium Pentagallide, PdGa5. *Z. Krist. - New Cryst. Struct.* **1997**, *212*, 6.
(53) Klimczuk, T.; Cava, R. J. Carbon Isotope Effect in Superconducting MgCNi3. *Phys. Rev. B* **2004**, *70*, 212514.
(54) Prozorov, R.; Kogan, V. G. Effective Demagnetizing Factors of Diamagnetic Samples of Various Shapes. *Phys. Rev. Applied* **2018**, *10*, No. 014030.
(55) Winiarski, M. J.; Wiendlocha, B.; Gołąb, S.; Kushwaha, S. K.; Wiśniewski, P.; Kaczorowski, D.; Thompson, J. D.; Cava, R. J.; Klimczuk, T. Superconductivity in CaBi2. *Phys. Chem. Chem. Phys.* **2016**, *18*, 21737−21745.
(56) McMillan, W. L. Transition Temperature of Strong-Coupled Superconductors. *Phys. Rev.* **1968**, *167*, 331−344.
(57) Jain, A.; Ong, S. P.; Hautier, G.; Chen, W.; Richards, W. D.; Dacek, S.; Cholia, S.; Gunter, D.; Skinner, D.; Ceder, G.; Persson, K. A. Commentary: The Materials Project: A Materials Genome Approach to Accelerating Materials Innovation. *APL Mater.* **2013**, *1*, No. 011002.
(58) Persson, K. *Materials Data on Ga9Rh2t*; Materials Project, 2020; DOI: 10.17188/1205583, accessed May 1, 2021.
(59) Ryżyńska, Z.; Chamorro, J. R.; McQueen, T. M.; Wiśniewski, P.; Kaczorowski, D.; Xie, W.; Cava, R. J.; Klimczuk, T.; Winiarski, M. J. RuAl6—An Endohedral Aluminide Superconductor. *Chem. Mater.* **2020**, *32*, 3805−3812.
(60) Peets, D. C.; Cheng, E.; Ying, T.; Kriener, M.; Shen, X.; Li, S.; Feng, D. Type-I Superconductivity in Al6Re. *Phys. Rev. B* **2019**, *99*, 144519.